Superconductivity and vortex phases in the two-dimensional organic conductor λ-$(BETS)_2Fe_xGa_{1-x}Cl_4$ ($x=0.45$)

S. Uji, T. Terashima, Y. Terai,* and S. Yasuzuka†
National Institute for Materials Science, Tsukuba, Ibaraki 305-0003, Japan

M. Tokumoto and H. Tanaka
National Institute of Advanced Industrial Science and Technology, and CREST JST, Tsukuba, Ibaraki 305-8568, Japan

A. Kobayashi
Research Centre for Spectrochemistry, Graduate School of Science, The University of Tokyo, Bunkyo-ku, Tokyo 113-0033, Japan

H. Kobayashi
Institute for Molecular Science and CREST JST, Okazaki, Aichi 444-8585, Japan
(Received 14 November 2004; published 31 March 2005)

Resistance measurements have been performed in a two-dimensional organic conductor λ-$(BETS)_2Fe_xGa_{1-x}Cl_4$ ($x=0.45$) to investigate the superconducting properties. In magnetic field parallel to the layers, the superconducting (S) phase is stabilized in a wide magnetic field range, which is qualitatively understood by Jaccarino-Peter compensation mechanism. Depending on the internal field created by the Fe 3d moments, three vortex phases in the S phase appear with increasing field; normal vortex, antivortex, and normal vortex phases. The superconducting transitions show characteristic field dependence, which is correlated to the vortex phases. In field perpendicular to the layers, the S phase appears only near the antiferromagnetic phase. The results for $x=0.45$ are also compared with those for the isostructural nonmagnetic salt $x=0$.

DOI: 10.1103/PhysRevB.71.104525 PACS number(s): 74.70.Kn, 71.18.+y, 71.20.Rv

I. INTRODUCTION

The discovery of the magnetic field induced superconductivity in the organic conductor λ-$(BETS)_2FeCl_4$, where BETS is bis(ethylenedithio)tetraselenafulvalene, has renewed the interest in the anisotropic superconductors.[1–3] In the absence of the magnetic field, λ-$(BETS)_2FeCl_4$ shows a transition from a paramagnetic metal (PM) to an antiferromagnetic insulator (AFI) around 8 K.[4–6] The AFI phase is destabilized by the magnetic field above ~10 T, and then the PM phase is recovered. The AFI ground state has been theoretically discussed in terms of the strong correlation effect.[7,8] When the magnetic field is applied parallel to the conduction layers, the superconducting (S) phase is stabilized between 18 and 42 T below 1 K.[1–3] This magnetic field induced S phase is destroyed when the field is tilted from the conduction layers. In contrast, the isostructural nonmagnetic salt λ-$(BETS)_2GaCl_4$ shows a superconducting transition ($T_c \approx 6$ K) at zero field.[5] The superconductivity is destroyed under magnetic field of 13 T parallel to the conduction layers.[9]

For the alloys λ-$(BETS)_2Fe_xGa_{1-x}Cl_4$, the PM-AFI transition is suppressed as x decreases, and then the ground state becomes superconducting for $x<0.35$ at zero magnetic field.[10] The global H-T phase diagrams of λ-$(BETS)_2Fe_xGa_{1-x}Cl_4$ in parallel fields ($H\|c$) have been also investigated.[11] As x decreases, the S phase simply shifts to a lower field whereas the AFI phase shrinks. The variety of the phases is apparently due to the x dependence of the effective exchange interaction between the Fe 3d magnetic moments and the π electron spins on the BETS molecules.

The overall features of the field-induced S phases in λ-$(BETS)_2Fe_xGa_{1-x}Cl_4$ are well understood by Fischer theory[12] based on Jaccarino-Peter (JP) effect.[13] In the PM phase of λ-$(BETS)_2FeCl_4$, the localized 3d moments are aligned along the external field (H). Because of a strong negative exchange interaction J between the 3d moments and the π electron spins, the π spins experience a strong internal field $-H_{\rm int}$ ($H_{\rm int}>0$) created by the 3d moments, whose direction is antiparallel to H. Therefore, the resulting field approaches zero when $H=H_{\rm int}$.[12] Under this condition, the Zeeman effect, one of the destructive mechanisms against superconductivity, is completely suppressed. When H is parallel to the conduction layers, the orbital effect, which is the other destructive mechanism, is also suppressed. Therefore, superconductivity can be induced by high parallel fields H in the order of $\sim H_{\rm int}$. The results of the Shubnikov–de Haas and angular-dependent magnetoresistance oscillations confirm their two-dimensional (2D) electronic states and the presence of the large internal fields.[14,15] When the field is tilted from the layers, the orbital effect works and the superconductivity is destabilized. As the Fe concentration x decreases, the average value of $H_{\rm int}$ decreases. This effect causes the field induced S phase to shift to a lower field.

In field induced superconductors due to the JP effect, the presence of a new vortex phase, an antivortex phase is theoretically predicted in a field range for $H<H_{\rm int}$.[16] For $H<H_{\rm int}$, the vortices carry paramagnetic currents instead of diamagnetic currents. The first evidence of such antivortices was obtained in the field induced S phase for a three-dimensional chevrel compound $Eu_{1-x}Sn_xMo_6S_8$.[16] A slight

increase of the magnetization due to the antivortices in addition to the large localized Eu magnetic moments is observed for $H<H_{\mathrm{int}}$. However, the effects of such antivortex formation on the transport properties have not been investigated so far.

In the alloy λ-$(BETS)_2Fe_xGa_{1-x}Cl_4$ ($x=0.45$), the superconductivity is stabilized in a wide field range between 0 and 25 T (Ref. 11) and both vortex and antivortex phases are expected to appear at relatively low fields. Therefore, λ-$(BETS)_2Fe_xGa_{1-x}Cl_4$ ($x=0.45$) may be one of the best systems to investigate such characteristic vortex phases realized by the JP effect. In this paper, we report anomalous behavior in the resistive transitions in λ-$(BETS)_2Fe_xGa_{1-x}Cl_4$ ($x=0.45$), which is closely related to the vortex phases. We also compare the results with those of the isostructural nonmagnetic salt ($x=0$).

II. EXPERIMENT

The single crystals of λ-$(BETS)_2Fe_xGa_{1-x}Cl_4$ were synthesized electrochemically.[5] The crystals are needlelike, elongating along the c axis. The conduction plane is the ac plane and the least conducting direction is the b^* axis. The resistance was measured by a conventional four-probe ac technique with electric current along the b^* axis. Four gold wires ($\phi 10$ μm) were attached to the samples by carbon paint. The experiments were made with a 14 T superconducting or 25 T resistive magnet at Tsukuba Magnet Laboratories, NIMS. The samples were rotated in field by a rotator with the resolution of about 0.05°.

III. RESULTS

Figures 1(a)–1(c) show the temperature dependence of the resistance for $x=0.45$ under magnetic fields. At zero magnetic field, as temperature decreases, the resistance decreases down to zero around 5 K and then steeply increases at 3.3 K. These are the PM-S and S-AFI transitions, respectively. The behavior is consistent with the result reported previously.[10] For $H\|b^*$ [Fig. 1(a)], we note that the resistance shows no sign of superconductivity above 6 T. The transition curves seem to simply shift to a lower temperature as the field increases. For $H\|c$ [Figs. 1(b) and 1(c)], the transition curves show characteristic field dependence. The superconducting transition first becomes sharp with increasing field up to 16 T. After that, the transition seems to become broad at higher fields. The resistance shows broad peaks above T_c for $H>12$ T. The S-AFI transition is not observed above 3 T for $T>1.7$ K. For comparison, we present the resistive transition curves for the nonmagnetic salt ($x=0$) in Fig. 2. For both field directions, $H\|b^*$ and $H\|c$, the transition curves monotonically shift to a lower temperature as field increases.

In Figs. 3(a) and 3(b), we present the T-H phase diagram for $x=0.45$. It is pointed out that there may be no apparent correct choice of criteria to unambiguously determine T_c or H_{c2} in resistance measurements.[17] In this paper, we simply define T_c when $R/R_n=0.5$, where R_n is the normal state resistance given by extrapolating the $R(H)$ curve from the high-temperature range. For $H\|b^*$, as the field increases, T_c steeply decreases down to 4 K and then lies just above the AFI phase boundary T_{AFI}. The superconductivity is stabilized up to 5 T at low temperatures. A similar behavior is already reported for $x=0.4$ by Zhang *et al.*[18] This critical field $H_{c2}=5$ T seems very large as compared with 2 T for $x=0$ at 1.5 K. The AFI phase is first more stabilized with increasing field and T_{AFI} has a maximum at about 0.5 T. After that, T_{AFI} monotonically decreases with field. For $H\|c$, T_c decreases down to 4 K and then becomes almost independent of field in the range between 4 and 20 T. After that, T_c decreases again. The value of T_{AFI} monotonically decreases with increasing field. These features are discussed later. Figure 3(c) shows the T-H phase diagram for $x=0$. The value of T_c shows a slightly positive curvature for the perpendicular field ($H\|b^*$), as observed in various layered superconductors. The results are consistent with those reported previously.[9]

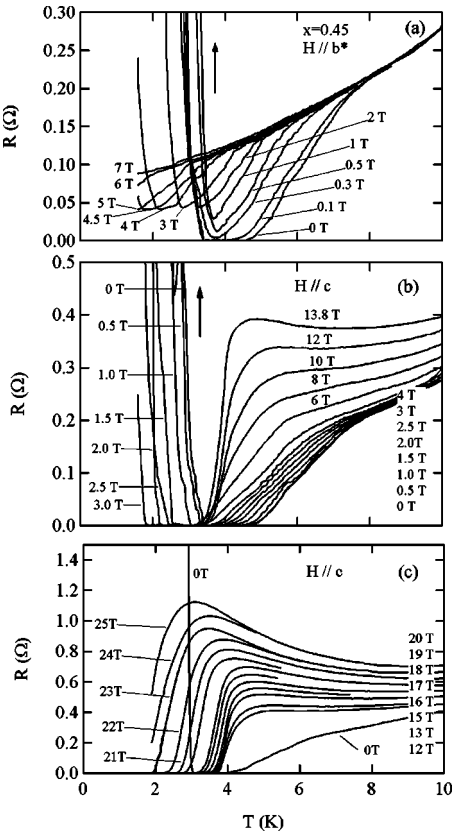

FIG. 1. Temperature dependence of resistance for (a) $H\|b^*$ and in (b) low and (c) high-field regions for $H\|c$ in λ-$(BETS)_2Fe_xGa_{1-x}Cl_4$ ($x=0.45$). The data in (a) and (b) are taken in the same run by use of a superconducting magnet. The data in (c) are taken for a different sample by use of a 25 T resistive magnet.

In Fig. 4, we plot the resistive transition width ΔT, which is defined as $\Delta T=T(R/R_n=0.9)-T(R/R_n=0.1)$. For $x=0.45$ [Fig. 4(a)], the field dependence of ΔT for $H\|b^*$ is not clear because of the limited field region. However, ΔT for $H\|c$ first has a maximum (~2.5 K) around 3 T and then decreases down to 0.5 K around 17 T. At higher fields, ΔT seems to increase again. For comparison, we present ΔT for $x=0$ in Fig. 4(b). In both field directions, we note that ΔT monotonically increases with increasing field.

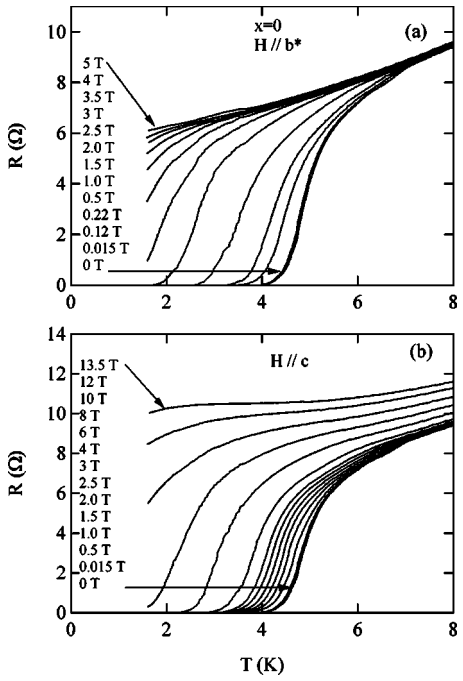

FIG. 2. Temperature dependence of resistance for (a) $H\|b^*$ and (b) $H\|c$ in λ-$(BETS)_2Fe_xGa_{1-x}Cl_4$ ($x=0$).

Figures 5(a) and 5(b) show the magnetic field angle dependence of the resistance at 3.25 K for $x=0.45$, where the field is rotated in the b^*c plane. For $H\|c$, the resistance has a steep decrease due to the superconducting transition. At 4 T, the superconducting transition is rather rounded, whose angular dependence is approximately given by a simple scaling function $R\sim|\cos(\theta)|^{\alpha}$. This scaling behavior suggests that the resistance depends only on the perpendicular component of the external field, i.e., the electronic state is highly two dimensional.[19,20] The exponent α decreases with increasing field and the curve at 8 T is well fitted with $\alpha\approx 1.0$. As the field further increases, the superconducting transition for $\theta\simeq 90°$ becomes sharp and peaks on both sides of the transition become evident as denoted by arrows. The peaks are visible up to 21 T and then rounded curves appear again at higher fields. The peak positions depend on field. The steep change of the resistance, deviating from the scaling $R\sim|\cos(\theta)|^{\alpha}$, suggests some phase transition. We have measured the resistance in the opposite field rotation, but found no appreciable hysteresis. For comparison, the results for $x=0$ are also shown in Fig. 5(c). We observe a similar resistance decrease due to the superconducting transition for $\theta\simeq 90°$. The transition is monotonically suppressed as the field increases as expected for conventional superconductors. The peaks on both sides are slightly visible even for $x=0$.

So far, similar peaks and step decrease of the resistance in parallel fields have been observed in high-T_c superconducting cuprates[21] and an organic superconductor.[22] They have been interpreted in terms of a vortex lock-in transition and/or flux flow resistance.[21,22] Although the interpretation is still somewhat controversial, it is likely that the results in these salts are caused by the vortex lock-in transition as discussed later.

Figure 6 presents the magnetic field angle dependence of the resistance at various temperatures for $x=0.45$. As shown

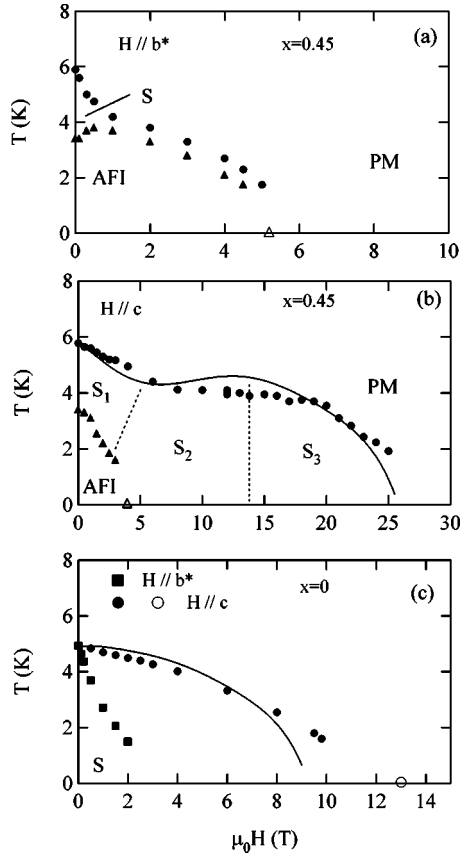

FIG. 3. T-H phase diagrams for (a) $H\|b^*$ and (b) $H\|c$ in $x=0.45$, and (c) in $x=0$. The closed symbols show the data from Figs. 1 and 2. The open symbols show the data determined from the magnetic field sweeps at 30 mK. The solid lines in (b) and (c) are calculated phase boundaries for $H\|c$ by Fischer theory. The dotted lines in (b) show the $M_s=0$ lines, dividing the S phase into three different vortex phases. See text for detail.

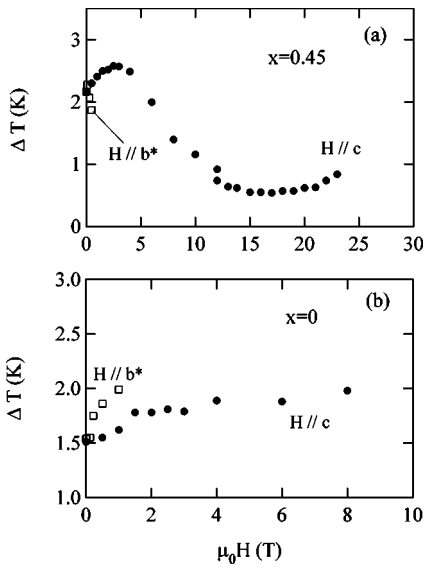

FIG. 4. Resistive transition width ΔT for (a) $x=0.45$ and (b) $x=0$.

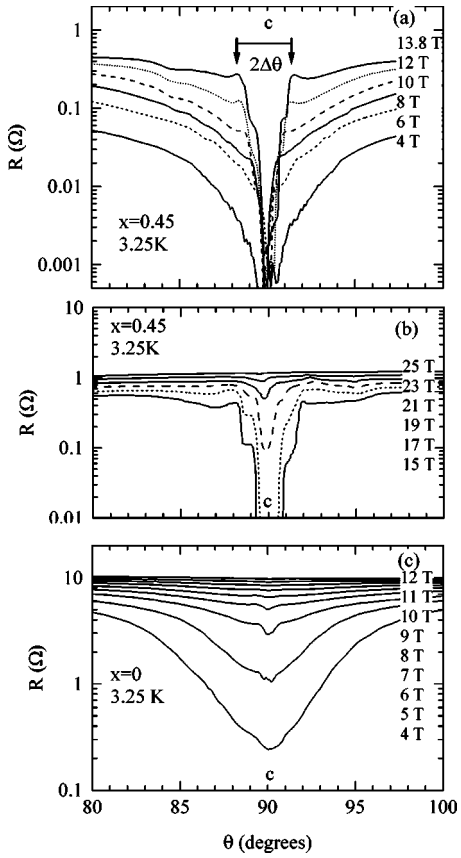

FIG. 5. Resistance as a function of the field angle θ in the b^*c plane for (a) and (b) $x=0.45$, and (c) $x=0$. The definition of $\Delta\theta$ is shown in (a).

in the inset, the peaks are evident in the range between 3.25 and 4.5 K. The peak positions slightly shift to 90° as temperature increases. Figure 7 presents the peak width $\Delta\theta$ at 3.25 K, defined in Fig. 5(a). For $x=0$, we note that $\Delta\theta$ has a tendency to decrease with increasing field. For $x=0.45$, however, $\Delta\theta$ increases with field, has a broad maximum around 17 T, and then seems to decrease. At high fields, the peaks are very rounded, so the data include large errors. This behavior seems correlated to the transition width ΔT shown in Fig. 4(a).

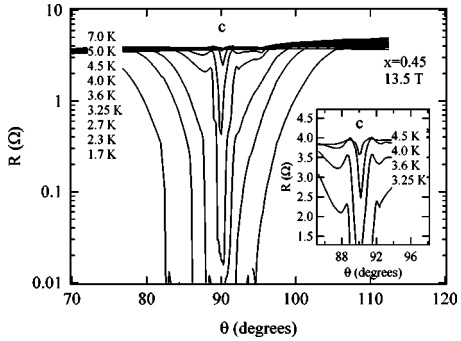

FIG. 6. Resistance as a function of the field angle θ in the b^*c plane for $x=0.45$. The inset shows the lock-in transition behavior near 90°.

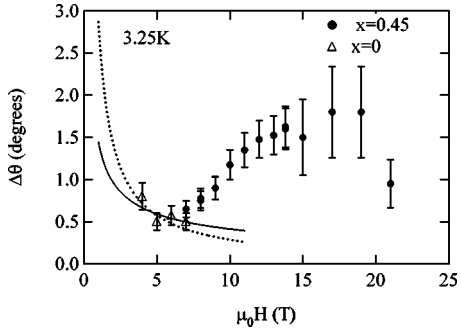

FIG. 7. The peak width $\Delta\theta$ at 3.25 K for $x=0.45$ and $x=0$. The solid and dotted lines are the calculated results. See text for detail.

IV. DISCUSSION

A. Phase diagram

The global H-T phase diagrams of λ-$(BETS)_2Fe_xGa_{1-x}Cl_4$ in parallel fields ($H\|c$) are qualitatively understood by Fischer theory[12] based on Jaccarino-Peter (JP) effect in 2D systems.[11] Fisher gave a full description for T_c and H_{c2} in the 2D case under fields along the conduction layers

$$\ln\frac{1}{t}=\left(\frac{1}{2}+\frac{i\lambda_{SO}}{4\gamma}\right)\Psi\left(\frac{1}{2}+\frac{h^2+i\lambda_{SO}/2+i\gamma}{2t}\right)+\left(\frac{1}{2}-\frac{i\lambda_{SO}}{4\gamma}\right)\Psi\left(\frac{1}{2}+\frac{h^2+i\lambda_{SO}/2-i\gamma}{2t}\right)-\Psi\left(\frac{1}{2}\right), \tag{1}$$

$$\gamma=[\alpha^2(h+h_J)^2-\lambda_{SO}^2]^{1/2}. \tag{2}$$

In the formula, reduced units are used: $t=T/T_c$, $h=0.53H_{c2}/H_{c2}^*$ and $h_J=0.53H_J/H_{c2}^*$. There are four adjustable parameters, the critical temperature T_c, the orbital critical field H_{c2}^*, the exchange field H_J whose field and temperature dependence is given by the Brillouin function, and the spin-orbit scattering parameter λ_{SO}. The scattering parameter due to magnetic impurities λ_m is taken to be zero for simplicity. Ψ is the digamma function. The value α is Maki parameter defined as $\alpha=\sqrt{2}H_{c2}^*/H_p$, where H_p is the Pauli limit.[23,24]

When the internal field $H_{\rm int}$ is sufficiently large, the low and high field S phases are well separated. However, when $H_{\rm int}$ is relatively small, both the S phases are merged into a single S phase. This is the case for $x=0.45$. The AFI phase inside the S phase is due to another mechanism.[7,8] The solid line in Fig. 3(b) shows the calculated result with the parameters $T_c=5.7$ K, $\mu_0H_{c2}^*=27$ T, the saturated value of the exchange field $\mu_0H_J^*=18$ T, and $\lambda_{SO}=6$. The field dependence of T_c has a maximum when the field $H=H_{\rm int}$. It should be noted that the internal field $H_{\rm int}$ is lower than the exchange field, $H_{\rm int}=H_J-1/\eta$, where $\eta\approx\alpha/\lambda_{SO}T_c$. We obtain that $H_{\rm int}=H_J$ in a pure 2D case because H_{c2}^* is infinite ($1/\eta=0$). The experimental result seems well reproduced by the theory. For comparison, we also show the calculated result for $x=0$ by the solid line in Fig. 3(c). The parameters for $x=0$ are $T_c=5$ K, $\mu_0H_{c2}^*=13$ T, $\mu_0H_J^*=0$ T, and $\lambda_{SO}=9$. The

smaller H_{c2}^{*} for $x=0$ shows that the Josephson coupling between the BETS layers is stronger. This tendency has been explained in terms of the Cooper pair tunneling via the empty 4*s* levels of the Ga^{3+}ions[2]. The smaller λ_{SO} for $x=0.45$ may be due to the better sample quality. For $x=0$, H_{c2} below 2 K is much larger than the fitted results, exceeding the Pauli limit. This behavior is first reported by Tanatar *et al.*[25] and the possibility of a superconducting state with spatially modulated order parameter is proposed.

When the JP effect works as in this case, the presence of a new vortex state, an antivortex phase, in a limited magnetic field range is predicted by Fisher *et al.*[16] They calculated the free energy with use of the Ginzburg-Landau theory, and obtained the magnetization M_s of the superconducting state, which does not include that of the localized magnetic moments. The condition for no vortices, $M_s=0$ ($H=H_{\rm int}$) is given by

$$1+\eta[H-H_J(H,T)]\left(1-\frac{dH_J(H,T)}{dH}\right)=0. \qquad (3)$$

When the low- and high-field *S* phases are merged into a single *S* phase as shown in Fig. 3(b), there are two solutions, which also correspond to the points at the boundaries where $dH_{c2}/dT=\infty$.[16]

In a high-field range, $H_J=$const, i.e., $dH_J/dH=0$, so we obtain $H=H_{\rm int}=H_J^{*}-1/\eta$. It gives a high field vortex phase boundary. In a low-field range where $H_{\rm int}$ is sufficiently low, we have another solution, giving a low-field boundary. Consequently, we have three vortex phases S_1, S_2, and S_3, whose phase boundaries are shown by the dotted lines in Fig. 3(b). In the S_1 phase, where $H_{\rm int}<H$, M_s is negative (the electronic state is diamagnetic). This is a normal vortex phase. In the S_2 phase ($H_{\rm int}>H$), M_s is positive, and an antivortex phase is realized.[16] In the S_3 phase, a normal vortex phase appears again because $H_{\rm int}<H$. These unique vortex phases are probably the main origin of the observed anomalous transition width and lock-in transition behavior as discussed later. The first experimental evidence of the presence of the antivortices was obtained in the field-induced *S* phase of the chevrel compound.[16] The magnetization was found to have a small paramagnetic component in addition to the large paramagnetism arising from the localized Eu moments. However, any anomalous features in the resistive transitions as observed in λ-$(BETS)_2Fe_xGa_{1-x}Cl_4$(=0.45) have not been reported in the chevrel compound.

For $H\|b^{*}$ [Fig. 3(a)], the orbital effect strongly works so that the superconductivity can not be stabilized in high fields. When the AF order is broken by the field, the 3*d* moments are almost aligned along the field. In this process, the internal and external fields are probably canceled out in the very limited field range, i.e., the Zeeman effect is suppressed. This is probably the reason why we observe the superconductivity stabilized just above the AFI phase boundary $T_{\rm AFI}$ (up to 5 T) as reported previously.[18]

B. Resistive transition width

The resistive transition broadening in highly 2D systems has been discussed in terms of flux flow,[26] order parameter phase jumps at Josephson junctions,[27–29] and superconducting fluctuation.[30] However, the major mechanism of the broadening is still controversial. Generally, the superconducting fluctuation is enhanced for short coherence length and is evident only near the transition temperature. Because of the relatively long coherence length and very broad transition width, it is unlikely that superconducting fluctuation effect is dominant for λ-$(BETS)_2Fe_xGa_{1-x}Cl_4$. In these experiments, the electric current is perpendicular to the layers ($I\|b^{*}$), so the flux lines (Josephson vortices in this case, as discussed later) are forced to move in the layers by Lorentz force for $H\|c$. Such flux flow should cause some energy dissipation, which makes the transition width broad. The number of the flux increases with the field, the transition width due to the flux flow should increase with field. This picture qualitatively explains the results for $x=0$ in Fig. 4(b).

At present, we can not conclude that only the flux flow is the mechanism of the transition width for $x=0$. However, it may be worthwhile to discuss the transition width for $x=0.45$ in terms of the above picture. As shown in Fig. 3(b), there exist two $M_s=0$ lines in the *T*-*H* phase diagram. Apparently, $M_s=0$ when $H=0$. Because of no flux (no vortices) for $M_s=0$, the width ΔT should have minima at the fields where $M_s=0$ if the flux flow is the dominant mechanism. The minima for $H=0$ and $H\approx 17$ T may be understood by the above picture. However, we have no minimum around 4 T but a maximum around 3 T. For $H=0$ and $H\approx 17$ T, the internal field $H_{\rm int}$ is zero and well saturated in the whole temperature range, respectively, i.e., $H_{\rm int}$ has no temperature dependence. In the field near the low-field $M_s=0$ line, however, $H_{\rm int}$ increases with decreasing temperature, following the Brillouin function. Therefore, as temperature decreases, the number of vortices or antivortices changes, whose motion may broaden the transition width. We notice that $\Delta T\approx 0.6$ K for $H\approx 17$ T is much smaller than 2.1 K for $H=0$. The result is not understood by the flux flow mechanism. At present, the reason is not clear.

C. Lock-in transition

For anisotropic superconductors,[32] the Ginzburg-Landau (GL) coherence lengths parallel and perpendicular to the conduction layers, $\xi_{\|}$ and $\xi_{\perp}$, are determined from the parallel and perpendicular upper critical fields $H_{c2\|}=\phi_0/2\pi\xi_{\perp}(T)\xi_{\|}(T)$ and $H_{c2\perp}=\phi_0/2\pi\xi_{\|}(T)^2$, where ϕ_0 is the flux quantum. For $x=0.45$, $\xi_{\|}$ and $\xi_{\perp}$ at 1.5 K are estimated to be 130 and 11 Å, respectively, if we take $H_{c2\|}=H_{c2}^{*}$. Since the length $\xi_{\perp}$ is shorter than the layer spacing $d=18$ Å, this system is modeled as a 2D superconductor.[31] It is known that a transition of flux line structures as a function of the magnetic field direction, a lock-in transition takes place for highly 2D superconductors, which are characterized by layered structures and short coherence length along the perpendicular direction. In magnetic fields sufficiently tilted from the layers, there exist conventional tilted flux lines or combined vortex structures made by Abrikosov (pancake) and Josephson vortices, which penetrate into the superconducting layers perpendicularly, and lie in the insulating layers, respectively. When the field becomes almost parallel to the

layers, a lock-in transition takes place: the Abrikosov vortices are excluded and only the Josephson vortices are stabilized. Since the motion of the Josephson vortices causes much less energy dissipation than that of the Abrikosov vortices, the resistance steeply decreases at the lock-in transition. Peaks may appear at the lock-in transitions because of the critical fluctuation effect. The lock-in transition has been reported in magnetic torque, ac susceptibility, or the resistance in high-T_c cupurates[21,33–36] and organic conductors[22,37,38] but the full detail of the interpretation still seems controversial. Feinberg and Villard consider the soliton lattice shape of the flux line core and obtain the critical angle θ_c where the lock-in transition takes place[39]

$$\sin(\theta_c) = \frac{1}{\pi}\left[2\alpha\frac{H^*}{H}\left(1+\epsilon^2\frac{H^*}{H}\right)\right]^{1/2}. \tag{4}$$

Here α and H^* are of the order of 0.5 and $H_{c1\perp}$, respectively. The anisotropic parameter of the superconductivity is defined as $\epsilon = H_{c2\parallel}/H_{c2\perp}$.

On the other hand, Bulaevskii *et al.* show that the lock-in transition occurs when the perpendicular component of the field exceeds a threshold field $H_{\rm th}$ which is independent of the field angle and less than $H_{c1\perp}$.[40] The critical angle θ_c is given by

$$\sin(\theta_c) = H_{\rm th}/H. \tag{5}$$

The solid and dotted lines are the fitted results for $x=0$ with Eqs. (4) and (5), respectively. Both theories predict a second order phase transition at θ_c, which is consistent with the observation of no hysteresis. The parameters are $\alpha=0.25$, $\mu_0 H^*=100$ G, $\epsilon=5$ in Eq. (4) and $\mu_0 H_{\rm th}=500$ G in Eq. (5). Both curves can reproduce the experimental data. Although $\mu_0 H_{c1\perp}$ has not been obtained experimentally, it should be comparable to $\sim$90 G in κ-(BEDT-TTF)$_2$Cu(NCS)$_2$ ($T_c \approx 10$ K) (Ref. 37) or $\sim$40 G in κ-(BEDT-TTF)$_2$I$_3$ ($T_c \approx 3.5$ K).[41] Therefore, the value of $\mu_0 H_{\rm th}=500$ G may be too large. The model by Feinberg and Villard may be more appropriate.

For $x=0.45$, the transition width $\Delta\theta$ has a maximum around 17 T for $H\|c$, where the external and internal fields are almost canceled out, i.e., there are few vortices. As the field is tilted from the c axis, the orbital critical field H^*_{c2} decreases, and consequently the internal field $H_{\rm int}=H^*_J-1/\eta$ decreases because $\eta \propto 1/H^*_{c2}$. It means that the number of the vortices or antivortices changes as the field is tilted. For highly 2D superconductors, the angular dependence of the critical field is given by[42]

$$\left|\frac{H_{c2}(\theta)\cos(\theta)}{H_{c2\perp}}\right| + \left(\frac{H_{c2}(\theta)\sin(\theta)}{H_{c2\parallel}}\right)^2 = 1. \tag{6}$$

The value of $H_{c2}(\theta)$ shows a cusp for $\theta \approx 90°$. If we take $H_{c2\parallel}=H^*_{c2}=27$ T and $H_{c2\perp}=5$ T, $H_{c2}(\theta)/H_{c2\parallel}$ is 0.98 for $\theta=89°$, where the lock-in transition is observed. This change approximately causes the reduction of $H_{\rm int}$ only by 0.16 T. This small reduction is consistent with no appreciable change of $H_{\rm int}$ in tilted fields for $x=0.47$.[43] Moreover, the decrease of the in-plane field by the tilt of $\sim 1°$ from the layers is only 0.2%. Therefore, the change of the Josephson vortex number within the lock-in transition region is negligibly small. The lock-in transition should be mainly caused by the field perpendicular to the layers. Since $H_{c1\perp}$ has the maximum value at the high field vortex phase boundary, the maximum in the width $\Delta\theta$ around 17 T is qualitatively consistent with the picture of the lock-in transition.

As the field approaches the critical field or as temperature increases, $\xi_\perp$ increases and becomes larger than the layer spacing d. Therefore, in such field or temperature ranges, the superconductivity can not be modeled as 2D and Josephson vortices do not exist. It explains the rounded curvatures for $\theta \simeq 90°$ at low and high fields in Fig. 5(b), and above 4 K in the inset of Fig 6.

V. SUMMARY

We obtained the T-H phase diagram for $H\|c$ and $H\|b^*$ in λ-(BETS)$_2$Fe$_x$Ga$_{1-x}$Cl$_4$ ($x=0.45$). For $x=0.45$, the S phase is stabilized in a wide field range up to 25 T for $H\|c$ whereas it can be stabilized only near the AFI phase boundary for $H\|b^*$. The analyses of the phase diagram based on Fisher theory show that the S phase can be divided into three vortex phases (two $M_s=0$ lines): normal vortex, antivortex, and normal vortex phases appear with increasing field. The superconducting transition width ΔT shows the minima at $H=0$ and around the high-field vortex phase boundary, where the vortices are absent. However, ΔT has the maximum around 3 T, where the number of the vortices changes with decreasing temperature. The value of ΔT at the high-field vortex phase boundary is much smaller than that at $H=0$. This behavior is still an open question. The field angle dependence of the resistance shows the lock-in transition, due to the highly 2D characters of the superconductivity. The field dependence of the critical angle $\Delta\theta$ is qualitatively interpreted by the field dependence of $H_{c1\perp}$, which has the maximum at the high field vortex phase boundary.

ACKNOWLEDGMENTS

This work was supported by a Grant-in-Aid for Scientific Research from the Ministry of Education, Culture, Sports, Science and Technology (Grant No. 15073225).

*Present address: Department of Materials Science, Osaka Prefecture University, Sakai, Osaka 599-8531, Japan.

†Present address: Faculty of Science, Osaka City University, Osaka 558-8585, Japan.

[1] S. Uji, H. Shinagawa, T. Terashima, T. Yakabe, Y. Terai, M. Tokumoto, A. Kobayashi, H. Tanaka, and H. Kobayashi, Nature (London) **410**, 908 (2001).

[2] L. Balicas, J. S. Brooks, K. Storr, S. Uji, M. Tokumoto, H.

Tanaka, H. Kobayashi, A. Kobayashi, V. Barzykin, and L. P. Gor'kov, Phys. Rev. Lett. **87**, 067002 (2001).
[3] S. Uji, H. Kobayashi, L. Balicas, and J. S. Brooks, Adv. Mater. (Weinheim, Ger.) **14**, 243 (2002).
[4] H. Kobayashi, H. Akutsu, E. Arai, H. Tanaka, and A. Kobayashi, Phys. Rev. B **56**, R8526 (1997).
[5] H. Kobayashi, H. Tomita, T. Naito, A. Kobayashi, F. Sakai, T. Watanabe, and P. Cassoux, J. Am. Chem. Soc. **118**, 368 (1996).
[6] L. Brossard, R. Clerac, C. Coulon, M. Tokumoto, T. Ziman, D. K. Petrov, V. N. Laukhin, M. J. Naughton, A. Audouard, F. Goze, A. Kobayashi, H. Kobayashi, and P. Cassoux, Eur. Phys. J. B **1**, 439 (1998).
[7] C. Hotta and H. Fukuyama, J. Phys. Soc. Jpn. **69**, 2577 (2000).
[8] O. Cepas, R. H. McKenzie, and J. Merino, Phys. Rev. B **65**, 100502(R) (2002).
[9] M. A. Tanatar, T. Ishiguro, H. Tanaka, A. Kobayashi, and H. Kobayashi, J. Supercond. **12**, 511 (1999).
[10] A. Sato, E. Ojima, H. Akutsu, H. Kobayashi, A. Kobayashi, and P. Cassoux, Chem. Lett. **27**, 673 (1998).
[11] S. Uji, T. Terashima, C. Terakura, T. Yakabe, Y. Terai, S. Yasuzuka, Y. Imanaka, M. Tokumoto, A. Kobayashi, F. Sakai, H. Tanaka, H. Kobayashi, L. Balicas, and J. S. Brooks, J. Phys. Soc. Jpn. **72**, 369 (2003).
[12] O. Fischer, Helv. Phys. Acta **45**, 331 (1972).
[13] V. Jaccarino and M. Peter, Phys. Rev. Lett. **9**, 290 (1962).
[14] S. Uji, H. Shinagawa, C. Terakura, T. Terashima, T. Yakabe, Y. Terai, M. Tokumoto, A. Kobayashi, H. Tanaka, and H. Kobayashi, Phys. Rev. B **64**, 024531 (2001).
[15] S. Uji, C. Terakura, T. Terashima, T. Yakabe, Y. Terai, M. Tokumoto, A. Kobayashi, F. Sakai, H. Tanaka, and H. Kobayashi, Phys. Rev. B **65**, 113101 (2002).
[16] O. Fischer, H. W. Meul, M. G. Karkut, G. Remenyi, U. Welp, J. C. Piccoche, and K. Maki, Phys. Rev. Lett. **55**, 2972 (1985).
[17] W. K. Kwok, U. Welp, K. D. Carlson, G. W. Crabtree, K. G. Vandervoort, H. H. Wang, A. M. Kini, J. M. Williams, D. L. Stupka, L. K. Montgomery, and J. E. Thompson, Phys. Rev. B **42**, 8686 (1990).
[18] B. Zhang, H. Tanaka, H. Fujiwara, H. Kobayashi, E. Fujiwara, and A. Kobayashi, J. Am. Chem. Soc. **124**, 9982 (2002).
[19] G. Blatter, V. B. Geshkenbein, and A. I. Larkin, Phys. Rev. Lett. **68**, 875 (1992).
[20] Z. Hao and J. R. Clem, Phys. Rev. B **46**, R5853 (1992).
[21] G. S. Okram, C. Terakura, S. Uji, H. Aoki, M. Xu, and D. G. Hinks, Physica C **356**, 115 (2001).
[22] M. Chaparala, O. H. Chung, Z. F. Ren, M. White, P. Coppens, J. H. Wang, A. P. Hope, and M. J. Naughton, Phys. Rev. B **53**, 5818 (1996).
[23] B. S. Chandrasekhar, Appl. Phys. Lett. **1**, 7 (1962).
[24] A. M. Clogston, Phys. Rev. Lett. **9**, 266 (1962).
[25] M. A. Tanatar, T. Ishiguro, H. Tanaka, and H. Kobayashi, Phys. Rev. B **66**, 134503 (2002).
[26] M. Tinkham, Phys. Rev. Lett. **61**, 1658 (1988).
[27] V. Ambegaokar and B. I. Halperin, Phys. Rev. Lett. **22**, 1364 (1969).
[28] G. Briceno, M. F. Crommie, and A. Zettl, Phys. Rev. Lett. **66**, 2164 (1991).
[29] F. Zuo, J. A. Schlueter, M. E. Kelly, and J. M. Williams, Phys. Rev. B **54**, 11 973 (1996).
[30] M. Hikita and M. Suzuki, Phys. Rev. B **39**, 4756 (1989).
[31] W. E. Lawrence and S. Doniach, *Proceedings of the Twelfth International Conference on Low Temperature Physics*, edited by E. Kanada (Academic, Kyoto, 1971), p. 361.
[32] M. Tinkham, Phys. Rev. **129**, 2413 (1963); F. E. Harper and M. Tinkham, *ibid.* **172**, 441 (1968).
[33] S. Uji, C. Terakura, T. Terashima, Y. Okano, and R. Kato, Phys. Rev. B **64**, 214517 (2003).
[34] M. Oussena, P. A. J. de Groot, R. Gagnon, and L. Taillefer, Phys. Rev. Lett. **72**, 3606 (1994).
[35] D. E. Farrell, S. Bonham, J. Foster, Y. C. Chang, P. Z. Jiang, K. G. Vandervoort, D. J. Lam, and V. G. Kogan, Phys. Rev. Lett. **63**, 782 (1989).
[36] B. Janossy, A. de Graaf, P. H. Kes, V. N. Kopylov, and T. G. Tononidze, Physica C **246**, 277 (1995).
[37] P. A. Mansky, P. M. Chaikin, and R. C. Haddon, Phys. Rev. Lett. **70**, 1323 (1993).
[38] P. A. Mansky, G. Danner, and P. M. Chaikin, Phys. Rev. B **52**, 7554 (1995).
[39] D. Feinberg and C. Villard, Phys. Rev. Lett. **65**, 919 (1990).
[40] L. Bulaevskii, A. Buzdin, and M. Maley, Phys. Rev. Lett. **90**, 067003 (2003).
[41] S. Wanka, D. Beckmann, J. Wosnitza, E. Balthes, D. Schweitzer, W. Strunz, and H. J. Keller, Phys. Rev. B **53**, 9301 (1996).
[42] M. Tinkham, Phys. Rev. **129**, 2413 (1963).
[43] S. Uji, C. Terakura, T. Terashima, T. Yakabe, Y. Terai, Y. Imanaka, S. Yasuzuka, M. Tokumoto, F. Sakai, A. Kobayashi, H. Tanaka, H. Kobayashi, L. Balicas, and J. S. Brooks, Physica C **388-389**, 611 (2003).